Project report:
Production and characterization of spin coated cellulose based, PM6:Y6, PM6:Y6: PyDMA solar cells

Filloretë Rrahmani, University of Prishtina - Hasan Prishtina, Kosovo

Supervizor: Elisabeth Erbes

DESY Summer Student Programme 2022

Hamburg, 07.08.2022

Abstract

In this research organic solar cells were produced by spin coating process. PM6:Y6 and PM6:Y6: PyDMA were used as active layers. Different analysis techniques were used for characterization of the active layer film. UV-VIS measurements were performed and based on the absorbance intensity the presence of active layers with an absorbance of 0.25 for PyDMA, 0.3 for PM6 and 0.55 for Y6 was determined. AFM measurements have shown an active layer thickness of 121 nm and GISAXS analysis, damage scan respectively, indicates for a homogeneous film which shows damage after 4.5 sec. Efficiency of 2.16% for PEDOT: PSS/PM6:Y6:PyDMA/PDINO solar cell was determined by IV measurements.

Contents

1. Introduction

Organic Solar Cells - OSC or organic photovoltaics have the ability of converting the light into direct current DC electricity and are popular in the field of solar cells due to their properties, low cost of manufacturing and different substrate deposition ability. [1] Thin layers of organic molecules have the ability of absorbing large amount of light based on the high optical absorption coefficient that they contain. Based on the production, organic solar cells are categorized in two types: small molecule OPV cells and polymer-based OPV cells. Small molecule OPV cells use molecules that absorb broadly in the visible and near-infrared range of the electromagnetic spectrum. Generally, strongly conjugated phthalocyanines, polyacenes are used for electron donor systems, whereas for electron acceptor systems are used perylene dyes and fullerenes. These devices are typically fabricated by vacuum deposition. Polymer-based organic cells use derived fullerenes as electron acceptor systems and long - chain molecular system as electron donors. For an effective charge transfer between the electrodes its necessary a continuous space through the donor and the acceptor phases. [2]

Based on the fact that the active layer determines the efficiency of the OSC it's very important the production and morphology of this layer. [3] Spin coating parameters, sample volume and annealing affect the organic solar cell efficiency.

Organic solar cells basted on cellulose nanopaper have shown and efficiency of over 16%. [4] Besides the advantages that OSC contain there are also some barriers such as long-time reliability, and inefficiency. In general view OSC are promising in the field of electricity production and compared with the silicon based solar cells OSC have the advantage of lightweight, low expenses for fabrication, they are flexible and transparent which leads to a wide application in walls, roofs and windows.

2. Methods and Instrumentation

2.1 UV-VIS Spectroscopy

UV-VIS Spectroscopy is an optical spectroscopy method that has been used in this project. It is based on the interaction between electromagnetic radiation and matter. The obtained spectra present the absorption of the ultraviolet light which corresponds to radiation with a wavelength of 160 to 400 nm and the visual or visible light which corresponds to a wavelength of 400-780 nm. The relationship between the degree of radiation absorption and the concentration of absorbing particles in the environment is expressed through Lambert Beer's law, which is expressed through the formula;

$A = \log I_i/I_t = \xi Cl$

Where A is the absorbance of the diluted solution, I_i presents the incident light intensity, I_t transmitted light intensity, C is the molar concertation of the solution, l is the cuvette width and ξ presents the molar absorptivity coefficient of the solution.

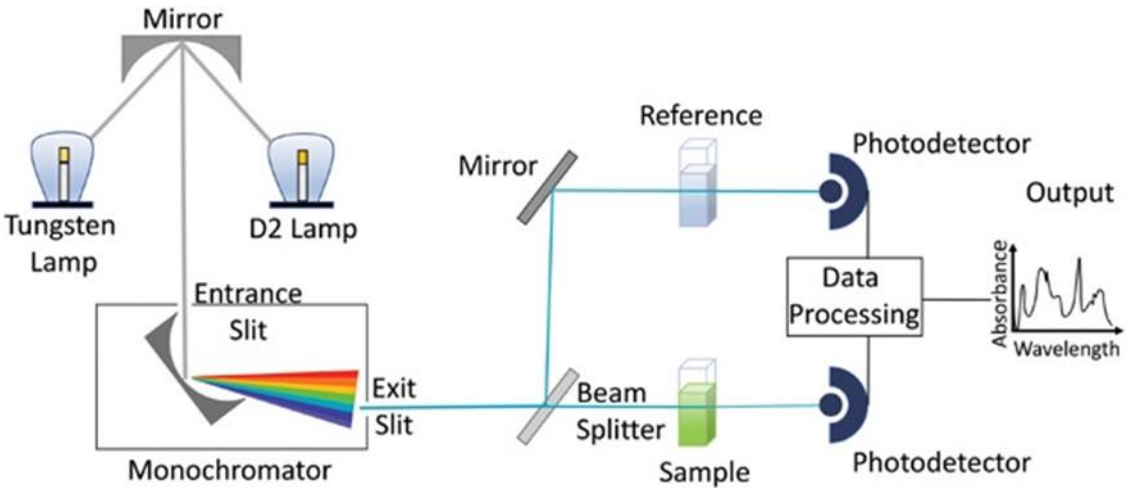

Fig.1 Schematic view of the UV-VIS spectrophotometer principle [5]

2.1.1 Radiation Sources

The radiation sources used for photometric measurements must meet three characteristics; have high radiation intensity in the entire area of photometric measurements, the radiation intensity should be constant with time and the beam of radiation to be homogeneous and parallel. It is important that the supply of the radiation source does not have fluctuations, as these current voltage fluctuations cause errors in photometric measurements. To avoid voltage fluctuations, stabilizers of the supply voltage of the radiation source are used. The most useful source for the infrared zone is the tungsten wire lamp, its emission spectral zone 320 to 2500nm. Sources of radiation for the ultraviolet region are gas discharge lamps such as hydrogen and deuterium discharge lamps which emit radiation in the 160 to 375 nm region.

2.2 Atomic force microscopy (AFM)

Atomic force microscopy (AFM) is a high-resolution non-optical imaging technique, advanced for analyzing the surfaces of the micro and nanostructured coatings and their interactions, further more by AFM measurement can be obtained information about optical, topography, magnetic, chemical and magnetic properties. [6]

A conventional AFM system with visual feedback operates primarily by scanning the AFM probe with a sharp AFM tip across a sample surface. The tip which can be made by silicon or silicon nitride is placed near the end of an AFM cantilever. The lateral and vertical positions of

the AFM probe with respect to the surface are controlled by a piezoelectric ceramic scanner. The deflection of the AFM cantilever varies when the AFM tip passes over objects of various heights. A laser beam is reflected from the rear of the AFM cantilever and directed into a position-sensitive photodetector in order to measure this deflection.

2.3 Organic Solar Cell IV Measurements

Power conversion efficiency (PCE) it the most important characteristic of the organic solar cell that represents the ability of the cell to convert light into electricity. Determination of the PCE is made by performing the IV measurements, where the cell is under illumination analogous to sun light and series of voltage are applied to the OSC. The IV curve is a product of the output current measured at each voltage step.

Pico AAA certified instrument was used for IV measurements that contained an integrated lamb for sun light illumination. Illumination was done with 1.5 G (1sun).

2.3.1 IV – Curve Parameters

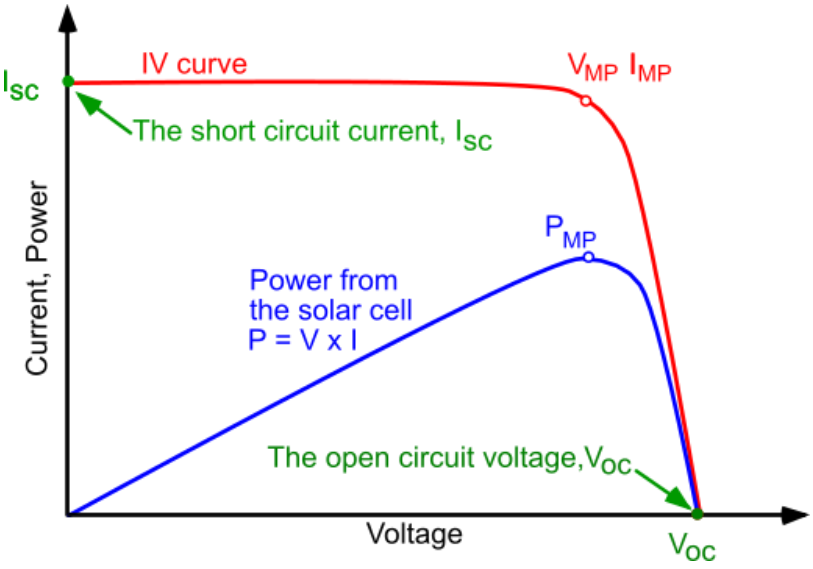

Fig.2 Current voltage curve of the solar cell [7]

The characteristic parameters form IV curves such as Isc, Voc, fill factor, efficiency, are used to characterize solar cells.

I_{SC} is the short-circuit current, that presents the current through the solar cell when the voltage over the SC is zero. I_{SC} depends from parameters such as: area of the solar cell, intensity and spectrum of the incident light, absorption and reflection of the solar cell and the minority-carrier collection probability which is related on the surface passivation.

V_{OC} is the open-circuit voltage, presents the maximum voltage of the solar cell, which arises at zero current.

FF is the abbreviation for the fill factor that presents the ratio between the maximum power P_{MP} from the solar cell to the product of the short-circuit current and open-circuit voltage.

Efficiency is the most frequently used parameter to evaluate how well organic solar cells perform. Efficiency shows the ratio of the solar cell energy output to solar energy input.

Efficiency of a solar cell depends from the temperature of the solar cell, intensity and spectrum of the sunlight, therefore the efficiency measurements should be obtained under standard conditions such as AM1.5 and a temperature of 25°C.

The efficiency of an organic solar cell is calculated by the equation as below:

$$\eta = \frac{V_{OC} \times J_{SC} \times FF}{P_{in}}$$

P_{in} is the input power that depends form the cell area and is $1kW/m^2$.

2.4 GISAXS - Principle

GISAXS stands for small angle x-ray scattering under grazing incident angles and is a method that is used to examine thin films, from micro to nanoscale surface and bulk structures. Based on the advantage of being a very fast technique and recording each scattering pattern just in few seconds, GISAXS overcomes the challenges that are carried by AFM such as limited scanning speed.

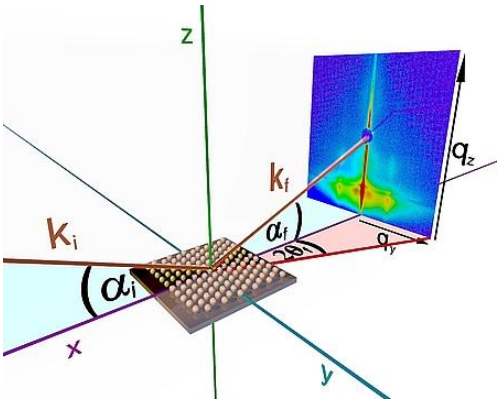

Fig.3 Schematic view of the GISAXS geometry [8]

The position of the sample is within the x,y, z coordinates and has an azimuthal orientation ω, α_i presents the incident angle whereas the exit angle is marked by α_f .The scattering plane is the (x,y) plane. So, the α_i is the angle under which the X-ray beam strikes the sample and exits by α_f angle. The incident angle should be around the critical angle of the film material of interest,

in order to get the structural information of the film. In order to protect the detector from damage that can be caused by the direct beam intensity and specular reflected beam, beam stoppers are used. For recording the scattered intensity, a 2-D detector is used. For GISAXS measurements the distance of the detector from the sample is in a range of 1 to 4 meters. [9,10,11]

For GISAXS measurements is necessary using a synchrotron radiation, the information that is obtained by the measurements needs to be translated to real space structural parameters because the detector records the Scattering in the reciprocal space. Grazing Incidence Small-Angle X-Ray Scattering (GISAXS) contains many advantages, starting form the fact that it's a non-destructive technique, gives information in a length range of micrometer to nanometer, can be used in different types of environments and also while *in situ* chemical reactions or catalytic reactions are taking place. Normally it does not require any specific sample preparation. [10]

3. Materials and methods

Organic solvents for substrate cleaning, acetone 99.5%, isopropanol 99% and ethanol 99% were purchased from Hofer Chemie, CG Chemikalien and VWR respectively. Special Glasses containing ITO and gold foil in the edges were sonicated for 15 minutes in the acetone bath after that each substrate was rinsed with isopropanol, ethanol and Mili-Q-water respectively. Each substrate was dried with nitrogen gas. Poly(3,4-ethylenedioxythiophene) polystyrene sulfonate - PEDOT: PSS 1.3% in H_2O was obtained by Sigma Aldrich. Ethyl lactate 98% was purchased from Bernd Kraft. 2,9-Bis[3-(dimethyloxidoamino)propyl]anthra[2,1,9-def:6,5,10-d'e'f']diisoquinoline-1,3,8,10(2H,9H)-tetrone - PDINO 98% was purchased from J&K Scientific. 1.6 mg/ml and 2.5 mg/ml of PDINO were diluted in ethyl lactate, sonicated in ultrasonic bath for 15 min in 30^{o}C and filtrated afterwards by 0.45µm PTFE syringe filter. PBDB-T-2F (PM6) and Y6 (BTP-4F) were purchased form Ossila. Pyrene-n,n-dimethylaniline (PyDMA) was obtained by Rare Chemicals GmbH. Chlorobenzene 99.5% was purchased from Roth and 1-chloronaphthalene from Sigma Aldrich. Active solutions were prepared by diluting PM6:Y6 in ratio (1:1.2) mg/ml and PM6:Y6: PyDMA in ratio (1: 1:0.2) or 29.08 mg of PM6 and 34.92 mg of Y6 for a total of 16mg/ml concentration in 4 ml volume of 99.5% ml chlorobenzene and 0.5% 1-chloronaphthalene and 29.08mg PM6, 29.08mg Y6 and 5.84mg for 16mg/ml of PM6:Y6: PyDMA. In each solution was added a magnetic stirrer and they were sonicated for one hour and left afterwards in the stirrer over night to dissolve completely.

3.1 Thin Film Deposition

The resistance of ITO film integrated in the substrates was measured by a multimeter and was around 2-50 Ω. The substrate was treated with air plasma pen for 2 minutes with a distance of 1 cm, the whole area was exposed to the plasma pen treatment, afterwards the following film was deposited within 5 minutes. 170µl of 1.3% PEDOT: PSS filtrated in 0.45 µm PTFE syringe filter was spin coated in the (20x25mm) substrate with spin coating parameters of 6000 rpm and 10 seconds, after that annealing at 150 ^{o}C under N_2 atmosphere took place. After first layer deposition the 2-step spin coating process was used for the active layer. 300 µL of PM6:Y6 was taken for a 20x25mm substrate and deposited with parameters as 500rpm, 10s for first step and 1500rpm and 40s for second step. Afterwards substrates annealed for 5 min at 100 ^{o}C under N_2 atmosphere. Last step was deposition of 300 µL PDINO dissolved in ethyl lactate.

Deposition of cellulose solution was performed by spraying set up at 100 ^{o}C for 10,20,30,40 and 50 cycles, waiting time between cycles 10 sec and 0.2 sec spraying time.

4. Results and Discussion

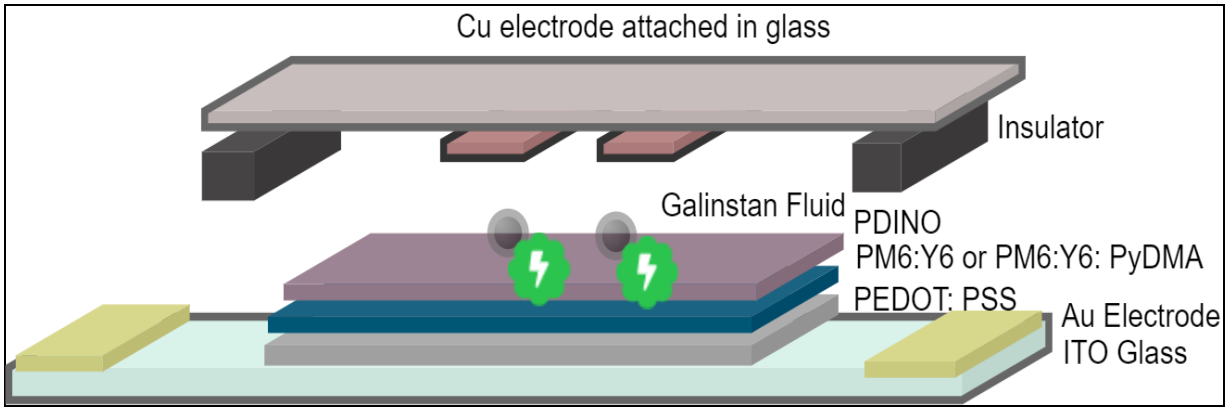

Fig. 4 Schematic view of organic layer deposition and organic solar cell construction

In figure 4 is represented the layer deposition in the ITO glass by spin coating process, the same procedure in done also by spraying setup, what is much more useful in terms of industry. The efficiency measurements were performed in that way that two wires connected to Cu and Au electrode and a voltage range from -6 to 6 V was applied in the cell and current intensity was measured.

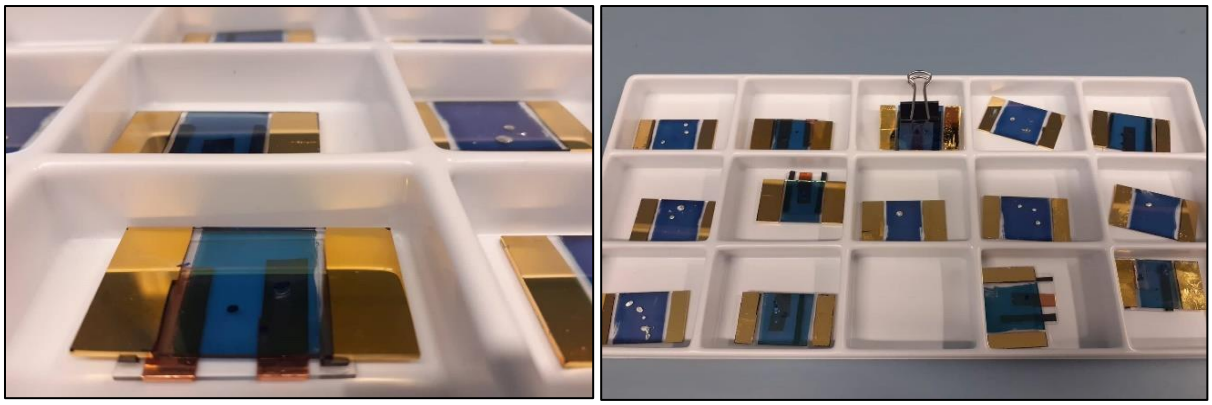

Fig. 5 Spin coated PEDOT:PSS/PM6:Y6/PDINO and PEDOT:PSS /PM6:Y6: PyDMA/PDINO solar cells

4.1 UV-VIS Spectra

In figure 5 are shown spin coated organic solar cells in the ITO glass first by using plasma pen for making a more hydrophilic surface followed by spin coating of 170 µL, 1.3% filtrated solution of PEDOT: PSS with spin coating parameters of 6000 rpm and 10sec followed by annealing for 10 min at 150 ^{o}C under N_2 atmosphere. Afterwards a two-step procedure was used for the deposition of the active layer PM6:Y6 or PM6:Y6: PyDMA in the ITO glass, first step 500 rpm, 10 sec and 1500 rpm, 40 sec second step followed by annealing for 5 min at 100 ^{o}C under N_2 atmosphere. After spin coated PDINO layer, solar cells were stored under N_2 atmosphere in the dark chamber.

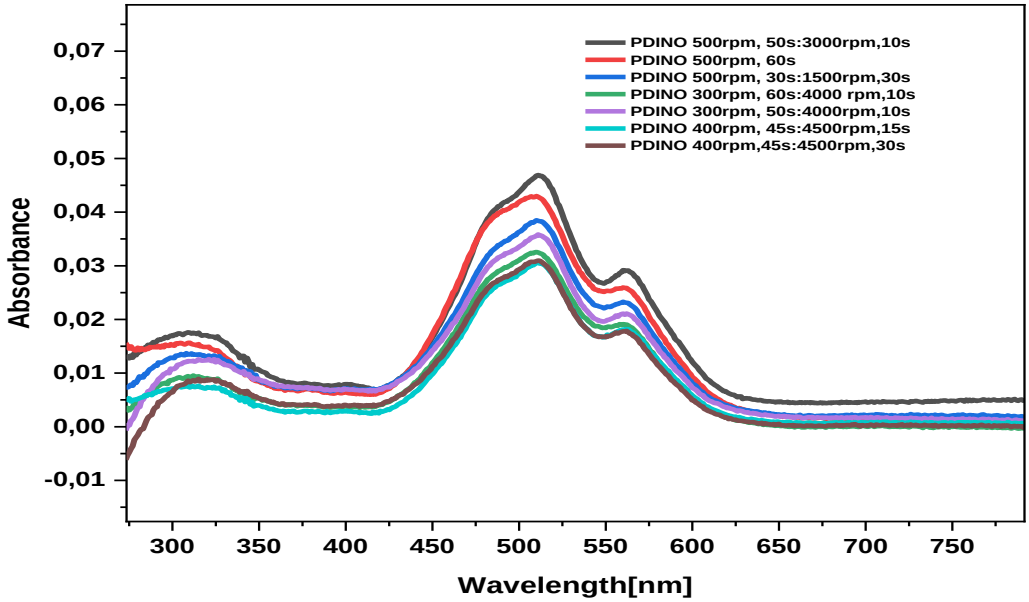

Graph 1. Indication of different spin coating parameters of PDINO- ethyl lactate in the intensity of the absorption peak

In the graph above is shown that 350 µL of 2.5 mg/mL PDINO, spin coated by two step procedure 500rpm, 50s and 3000rpm, 10s shows the highest intensity of absorbance when compared to other PDINO films, deposited with different parameters.

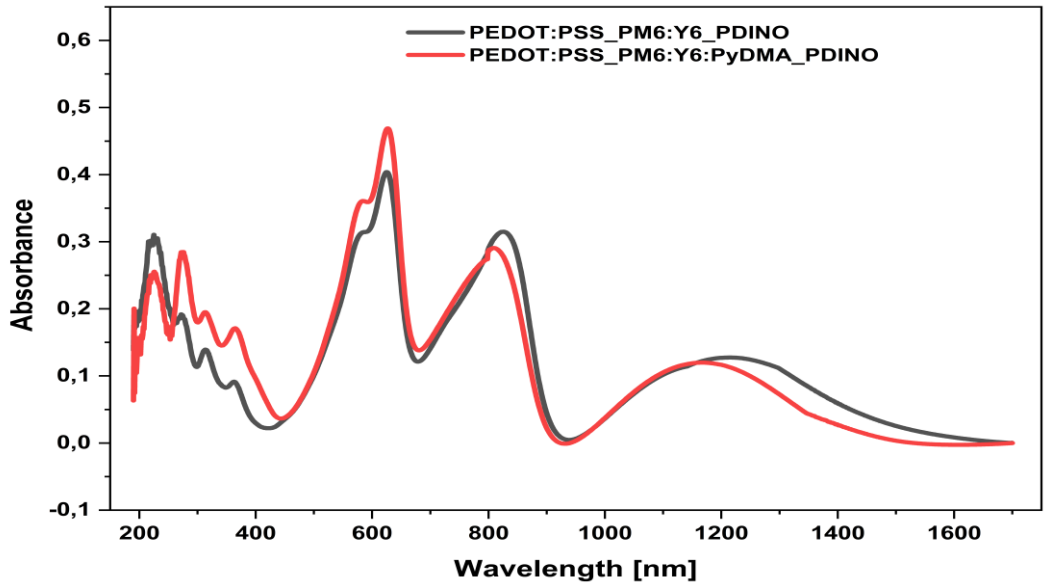

Graph 2. Absorption spectra of PEDOT:PSS_PM6:Y6 and PEDOT:PSS_PM6:Y6:PyDMA in the presence of PDINO

In the graph above is presented the comparison of absorption spectra for PEDOT:PSS_PM6:Y6_PDINO and PEDOT:PSS_PM6:Y6:PyDMA_PDINO, where the absorption peak for PEDOT:PSS_PM6:Y6:PyDMA_PDINO shows an lightly increasement in the light absorption when compared to the other active layer. The peak at ~ 300nm comes from the absorption of PyDMA, PM6 absorbs at ~ 590nm and Y6 at ~ 690nm and the broad peak at ~1200 nm is due to the presence of J aggregates that are many in the structures of the active layers.

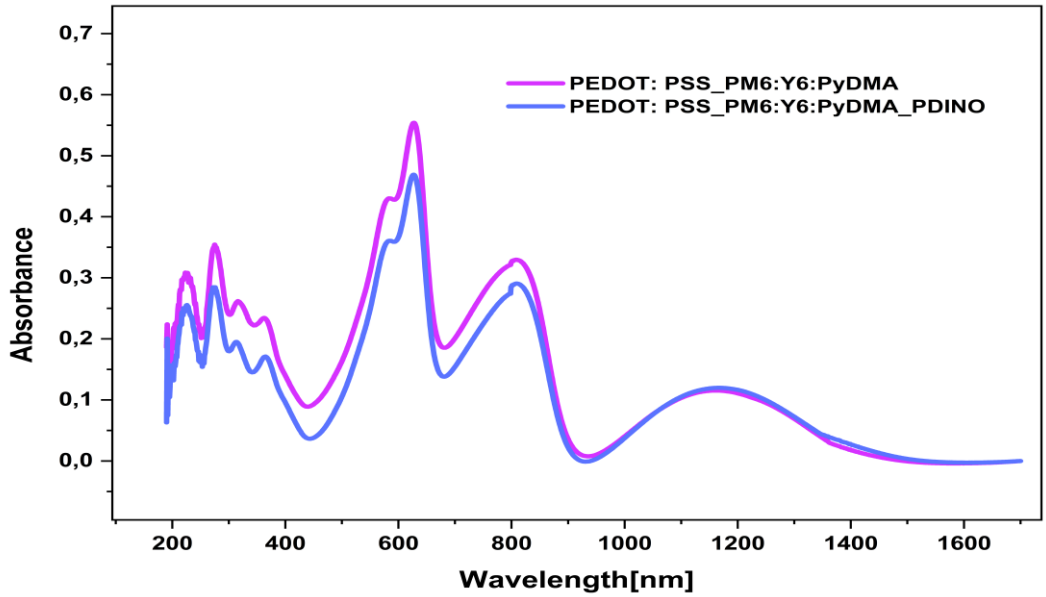

Graph 3. Absorbance spectra of 16mg/ml PEDOT: PSS_ PM6:Y6: PyDMA and in the presence of PDINO

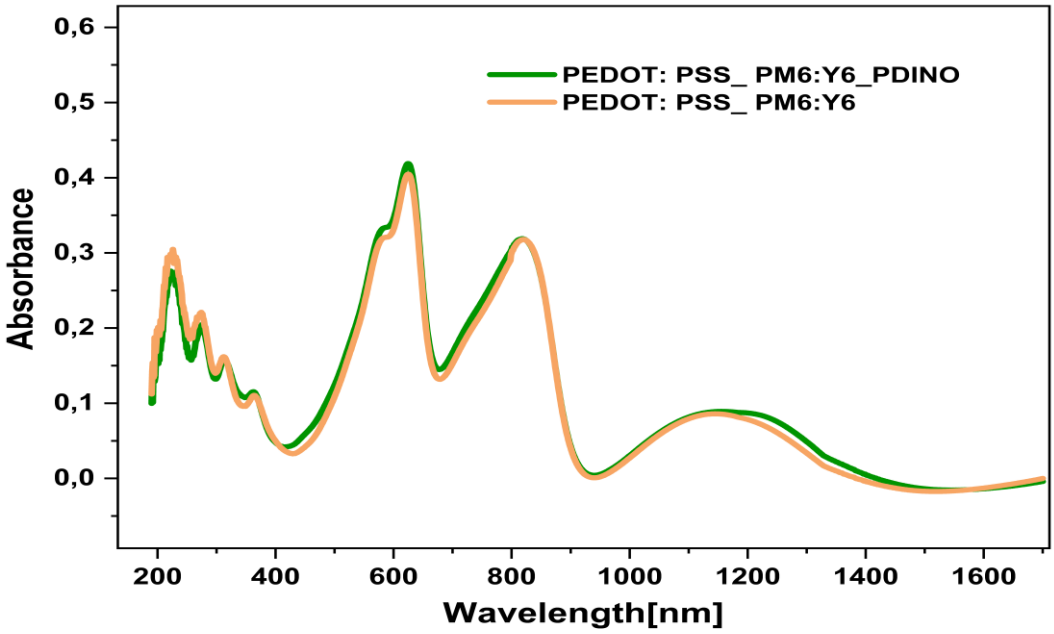

Graph 4. Absorbance spectra of 16mg/ml PEDOT: PSS_ PM6:Y6 and in the presence of PDINO

In the graph 3, the compared spectra of PEDOT: PSS_PM6:Y6:PyDMA and PEDOT:PSS_PM6:Y6:PyDMA_PDINO are shown. This indicates an increasement in the absorption intensity in the presence of PDINO whereas in graph 4 in case of PEDOT: PSS_PM6:Y6 and PEDOT: PSS_PM6:Y6:PDINO is not shown any change when PDINO is present.

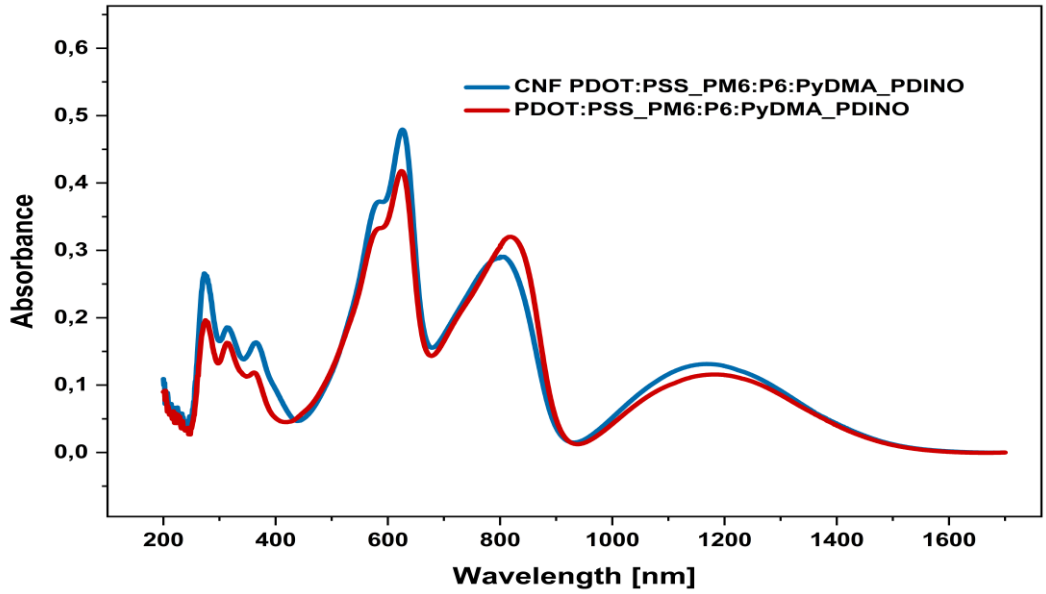

Graph 5. Absorbance spectra of PEDOT:PSS_ PM6:Y6:PyDMA in addition of 50 cycles sprayed cellulose

Form the compared graphs above can be concluded that addition of cellulose with spraying parameters of 0.2 sec spraying time and 50 cycles in total, has shown a growth for the light absorbance intensity.

4.2 IV- Curve and Efficiency

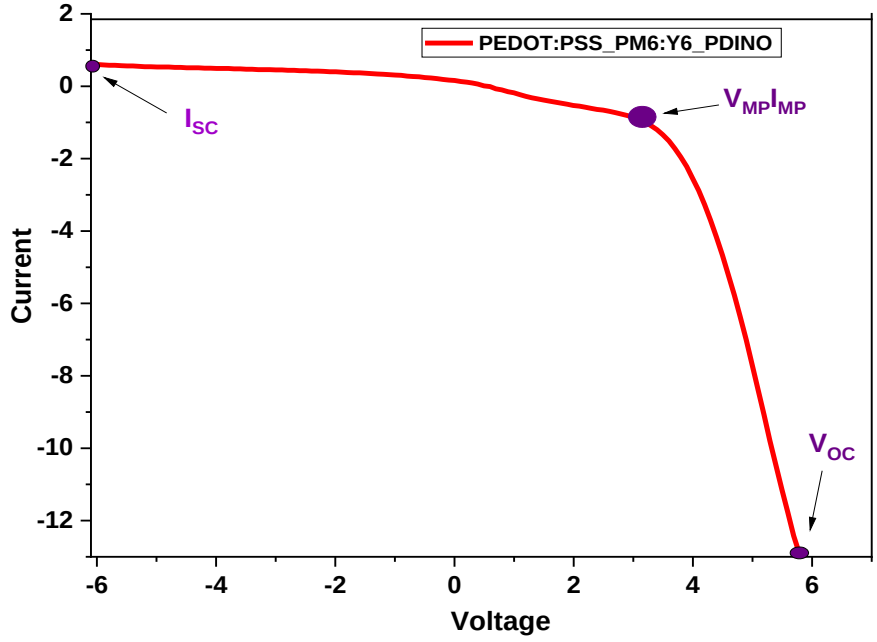

Graph 6. IV curve for PEDOT:PSS_PM6:Y6_PDINO

The measured parameters by IV measurements are:

Voc: 0.546 V, Isc: 0.16 mA, Im: 0.09 mA, Vm: 0.297 mA, FF: 30.56%, Shunt R: 8572.5 Ohms. Based these parameters efficiency of the PEDOT: PSS_PM6:Y6_PDINO organic solar cell can be calculated. The average area used was 0.07 cm^2.

$$\eta = \frac{V_{OC} \times J_{SC} \times FF}{P_{in}}$$

*Ƞ=0.546V*0.16mA*0.3056/1.779mW*

***η*=1.5%**

Efficiency of different active layers

Active layer	Efficiency
PEDOT: PSS_PM6:Y6:PyDMA_PDINO	2.16%
PEDOT: PSS_ PM6:Y6_PDINO	1.5%
CNF PE.PSS/ PM6:P6:PyDMA/PDINO	1.65%

4.3 GISAXS Data

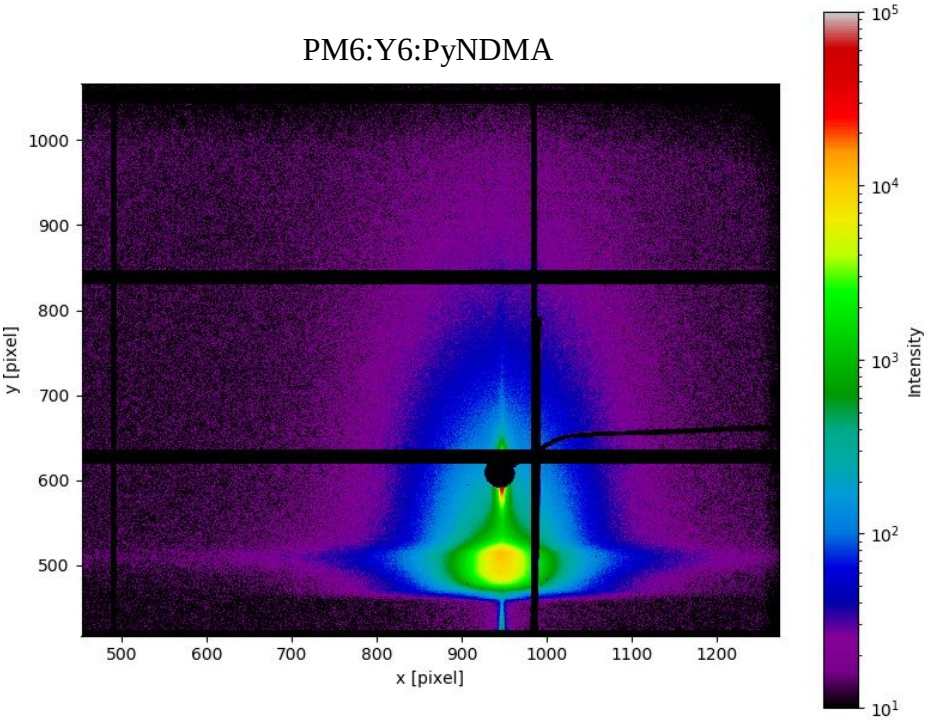

Fig.6 GISAXS scattering pattern of PM6:Y6: PyNDMA

From GISAXS experiments information about the structural composition of the sample can be obtained. In the figure above the information about the structure can be gained in the range of 500 pixels. We used an energy of 1.048nm, an incident angle of 0.37° and a sample to detector distance of 3.9m.

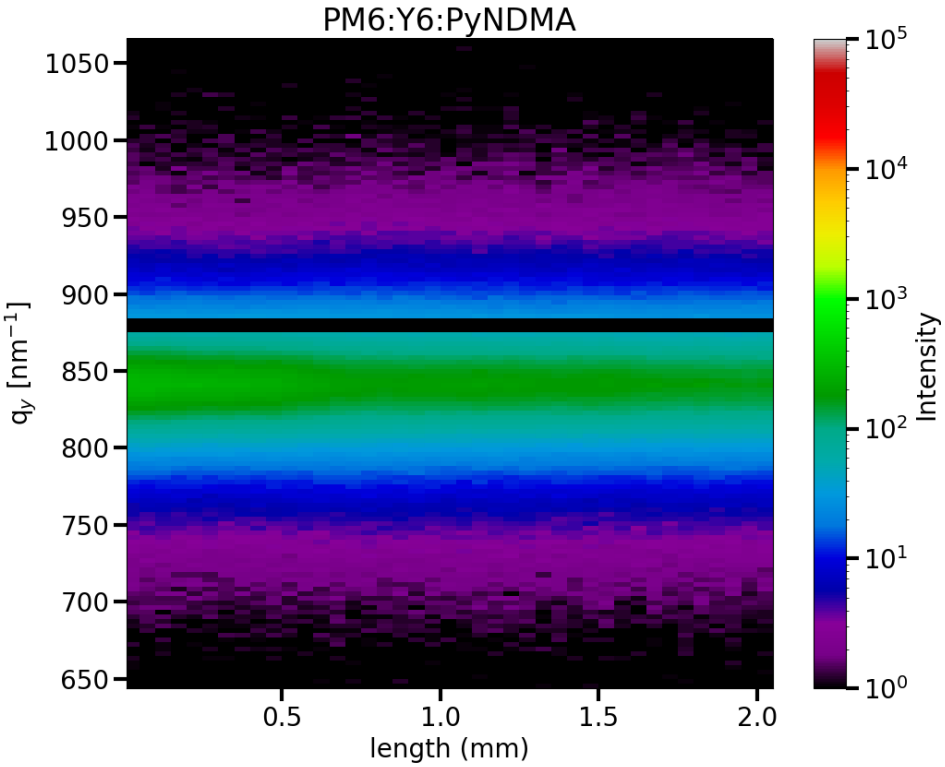

Fig.7 Homogeneity of PM6:Y6: PyNDMA

In the figure above the scattering intensity has not changed significantly over the lateral scan in qy direction, indicating a high homogeneity of the active layer film.

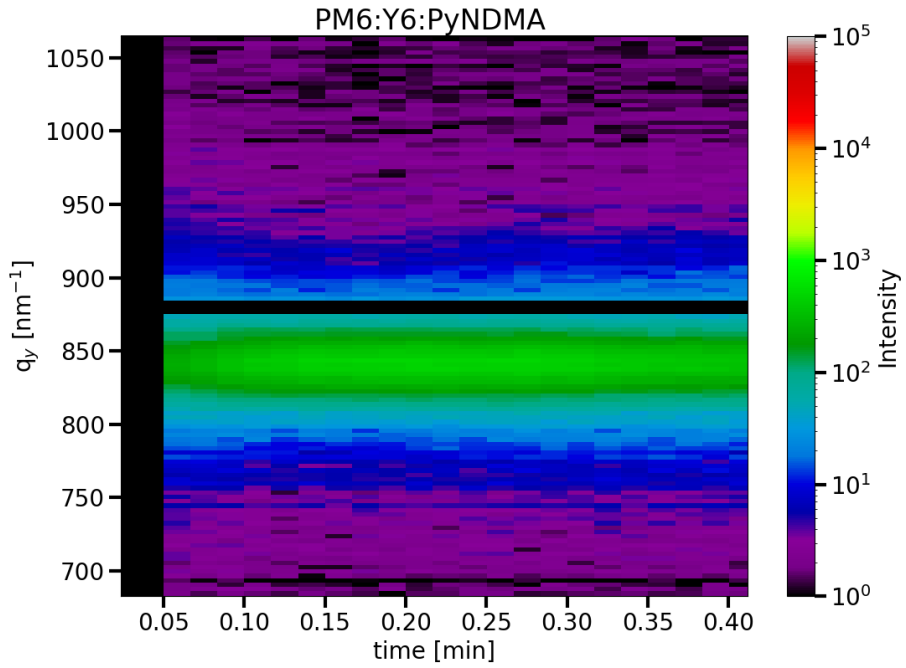

Fig.8 Damage scan of PM6:Y6: PyNDMA

Based on the figure 8 where the structure of the sample is showing characteristic changes can be concluded that the damage of the sample happening after 4.5 seconds.

4.4 AFM-Thickness Determination

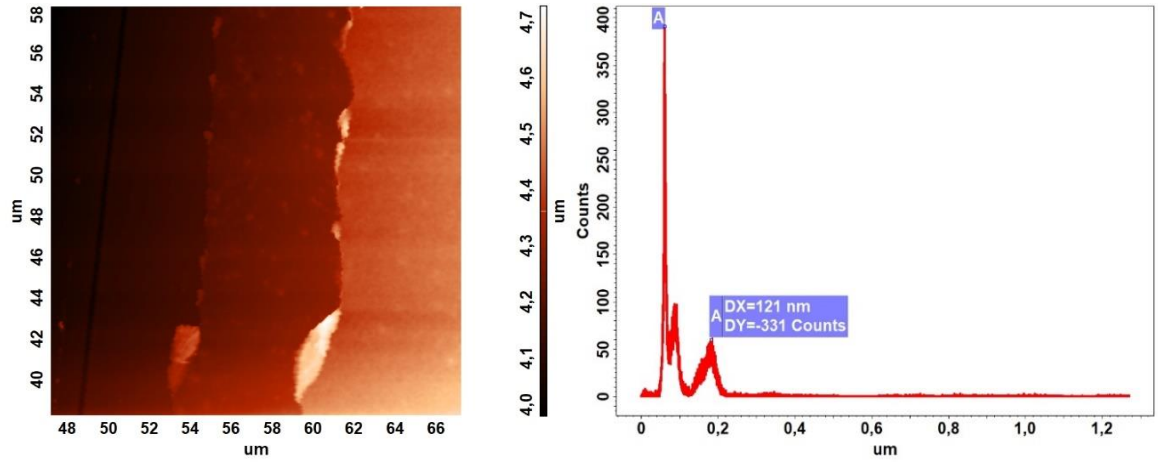

Fig.9 AFM images of PM6:Y6:PyDMA thin film on silicon substrate, spin coated by 2 step process of 500 rpm, 10 sec and 1500 rpm, 40 sec followed by annealing at 100 ^{o}C under N_2 atmosphere.

In fig.9 is shown the AFM height profile image of the active layer and the thickness which is found to be 121 nm for the PM6:Y6:PyDMA. After normalization to the silicon substrate, we can measure the thickness in the histogram of the height profile (fig. 9, right).

5. Conclusions

PM6:Y6, PM6:Y6: PyDMA cellulose based solar cells were produced and characterized by UV/VIS measurements that support the presence of the active layer for PyDMA absorption at ~ 300nm, PM6 at ~ 590nm and Y6 at ~ 690nm. IV measurements were conducted and the organic solar cell is found to be 2.16% for PEDOT: PSS PM6:Y6:PyDMA_PDINO, 1.5% for PEDOT: PSS_ PM6:Y6_PDINO and 1.65% for CNF PEDOT:PSS. PM6:Y6:PyDMA PDINO. 1.65%. Based on the AFM generated data, was found that the PM6:Y6:PyDMA thickness is 121nm. GISAXS measurements were performed and the taken results prove that the deposited layer of PM6:Y6:PyNDMA has a high homogeneity and based on the damage scan can be stated that the damage of the sample occur after 4.5 seconds.

Acknowledgements

I would like to express my gratitude to my supervisor Elisabeth Erbes for her guidance, encouragement and feedback during this project.

Additionally, thank you to the Summer Student Program organizers for this wonderful program and opportunity.

Finally, thank you to all the summer students for the cultural diversity that represented, that increased the value of the program.

References:

[1] Augustin McEvoy, Tom Markvart, Luis Castaner. Practical Handbook of Photovoltaics (Second Edition) Fundamentals and Applications 2012. Pages 543-569

[2] BlendsSvante Nilsson, Andrzej Bernasik, Andrzej Budkowski, and Ellen Moons. Morphology and Phase Segregation of Spin-Casted Films of Polyfluorene/PCBM

[3] Tracey M. Clarke,Amy M. Ballantyne,Jenny Nelson,Donal D. C. Bradley,James R. Durrant. Free Energy Control of Charge Photogeneration in Polythiophene/Fullerene Solar Cells: The Influence of Thermal Annealing on P3HT/PCBM Blends

[4] Junying Wu,a Xinpeng Che,b Hui-Chao Hu, Huimin Xu,a Bin Li, Yanjun Liu,a Jianguo Li,a Yonghao Ni, Xingye Zhanga and Xinhua Ouyang. Organic solar cells based on cellulose nanopaper from agroforestry residues with an efficiency of over 16% and effectively wide-angle light capturing.

[5] UV Spectroscopy- Definition, Principle, Parts, Uses [internet] Hamburg: DESY; [cited: 05.08.2022] Available from: https://thechemistrynotes.com/ultraviolet-visible-uv-spectroscopy.

[6] M. Aliofkhazraei, N. Ali. AFM Applications in Micro/Nanostructured Coatings.

[7] Short-Circuit Current [internet] Hamburg: DESY; [cited: 05.08.2022] Available from: https://www.pveducation.org/pvcdrom/solar-cell-operation/short-circuit-current

[8] GISAXS - Grazing Incidence Small Angle X-ray Scattering [internet] Hamburg: DESY; [cited: 06.08.2022] Available from: http://www.gisaxs.de/theory.html

[9] T.A. Ezquerra M.C. Garc´ıa-Gutierrez ´ A. Nogales M.A. Gomez (Eds.).

Applications of Synchrotron Light to Scattering and Diffraction in Materials and Life Sciences

[10] Gilles Renauda,∗ , Rémi Lazzari b , Frédéric Leroyc. Probing surface and interface morphology with Grazing Incidence Small Angle X-Ray Scattering

[11] S. Lenz1, M. Bonini2, S.K. Nett1,3, M.C. Lechmann1, S.G.J. Emmerling1, R.S. Kappes1, M. Memesa1, A. Timmann4, S.V. Roth4, and J.S. Gutmann1,3,a .Global scattering functions: a tool for grazing incidence small angle X-ray scattering (GISAXS) data analysis of low correlated lateral structures.